Portable Multi-Channel Electrotactile Haptic Feedback System

Team 2 — Jesse Cornman and Vikram Mudaliar

ECE 445 Final Report — Spring 2017

TA: John Capozzo

Abstract

No commercially-available upper limb prosthetic device provides expressive touch feedback. Lack of touch feedback is one of the most fundamental problems with modern myoelectric prosthetic devices [1], [2]. Because of this problem, users can’t grasp delicate objects without crushing them or feel anything they touch with their prosthetic hand, leading to reduced device embodiment, increased difficulty of use for manipulation, and increased device abandonment [3]. Our solution to this problem is to provide touch feedback by non-invasively stimulating nerves with electrical pulses, the intensity of which corresponds to pressure acquired from low-cost pressure sensors embedded in a prosthetic finger.

Table of Contents

1. Introduction

The work in this project stems from research performed by the Bretl Research Group, and the company PSYONIC. Our work is designed to be a subsystem of PSYONIC's robotic prosthetic hand, which uses electromyographic signals controlled by an amputee alongside machine learning algorithms to control the configuration of a robotic hand. Our project is designed to integrate into that hand, and consists of two major components: 1) tactile pressure sensing and 2) haptic feedback through electrical stimulation.

Common forms of tactile feedback for prosthetics include vibrotactile stimulation (small vibrating motors placed on the skin), non-invasive electrotactile stimulation, or invasive direct nerve stimulation. The two most viable techniques for a conventional myoelectric prosthetic are vibrotactile stimulation, and non-invasive electrotactile stimulation [4]. Non-invasive electrotactile stimulation has a number of advantages over vibrotactile stimulation, including spatial resolution, device longevity, and flexibility in sensation quality and intensity. However, due to size, cost and power limitations nearly all conventional electrotactile stimulators are used exclusively in research; there are currently no commercial prostheses which use electrotactile stimulation as a form of sensory feedback. Commercially-available constant current stimulators do exist, but are either expensive, energy inefficient, or large. An example of a device with similar performance specifications to ours is the BIOPAC STMISOLA, which costs approximately $1500, consumes almost 3W quiescent power, is too large to be mobile, and provides only one channel of stimulation. Our device is significantly smaller, more energy efficient, and can provide three channels of stimulation with pressure feedback at nearly 1/15th of the cost.

Pressure sensing in robotic applications is currently an area of active research. There are a number of different methods used, including the use of fluids, capacitive sensors, and piezoelectric resistors. Most methods are either too expensive to be viable or too low-performance to be useful. A pressure sensing method which provides a good compromise between performance and cost is the use of barometric pressure sensors sealed in silicone, a technique employed by the companies TakkTile and PSYONIC. We improved on this design by mounting an array of barometric sensors on a flexible PCB, allowing the device to easily mount and conform to a compliant robotic finger.

2. Design

2.1 Block Diagram

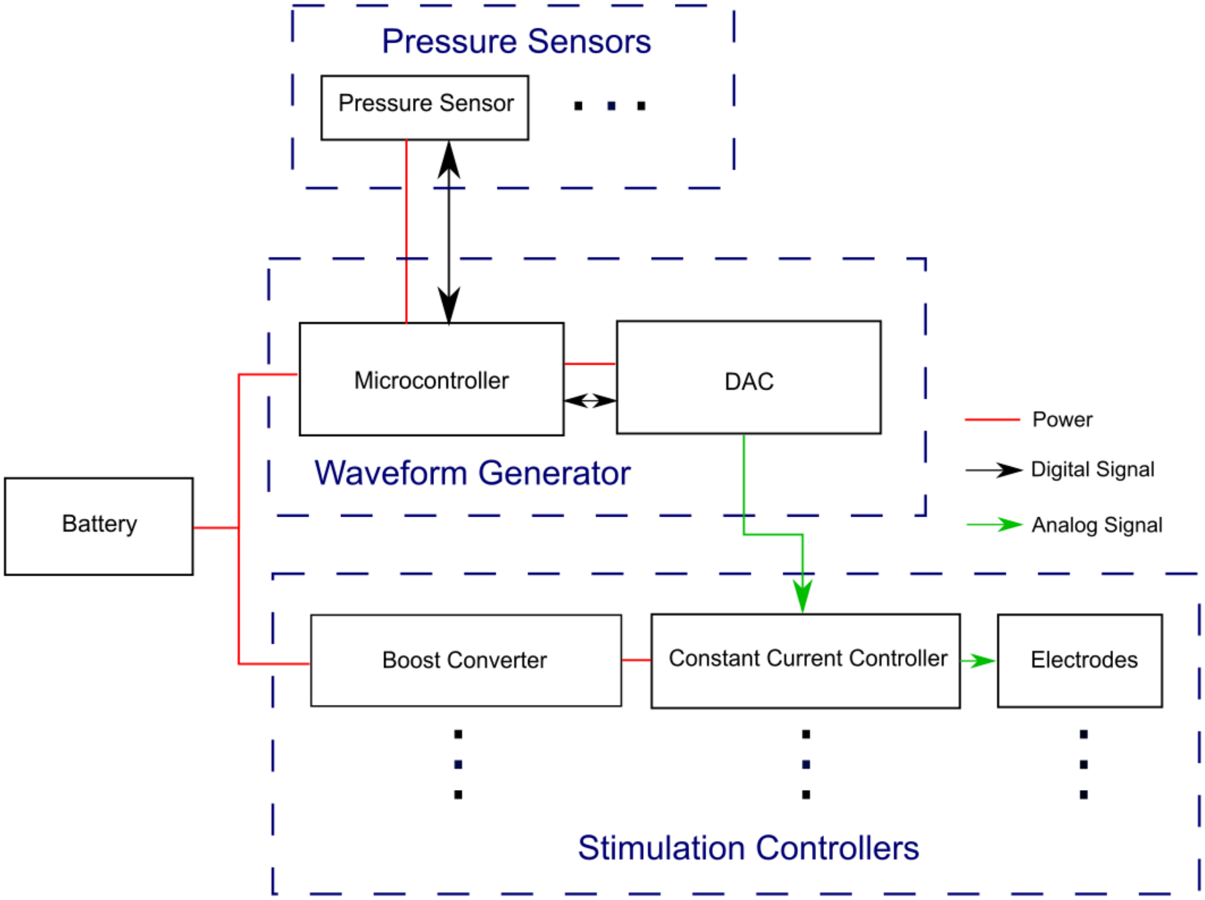

Figure 1. Block Diagram

The stimulator consists of four different primary modules: the digital to analog converter (DAC), the high voltage power converters, the pressure sensors, and the analog constant current controllers. The relationship between these modules is shown in Figure 1. The DAC module is comprised of a microcontroller and an eight channel SPI DAC chip. The power supplies convert a battery voltage (between 9-11.1V_{dc}) to between +/-200-300V_{dc}, to power the constant current controller. The pressure sensors are arranged in clusters of up to three, and interface with I2C muxes. The constant current controller outputs a current which varies as a linear function of the voltage output from the DAC. The stimulator provides constant current stimulation with a compliance voltage of +/-150V across the user's skin. Constant current is superior to constant voltage for this application because it helps maintain a consistent sensation when electrodes shift and protects the device if the electrodes short [5]. The output of the device is "arbitrary waveform," meaning that it is able to accurately track reference voltages quickly and with minimal distortion. Waveform shape can change the perceived quality of the stimulation, so having this requirement allows for future research in sensation quality control. For testing purposes however, we deliver only 'biphasic' square pulses, which are a standard for electrotactile stimulation. The amplitude of these pulses varies as a function of the measured pressure on the corresponding channel. The overall design is modular; the DAC has eight ports which connect to current controller/high voltage power supply modules, and a port for I2C which allows for multiple addressable pressure sensor boards.

2.2 Constant Current Controller

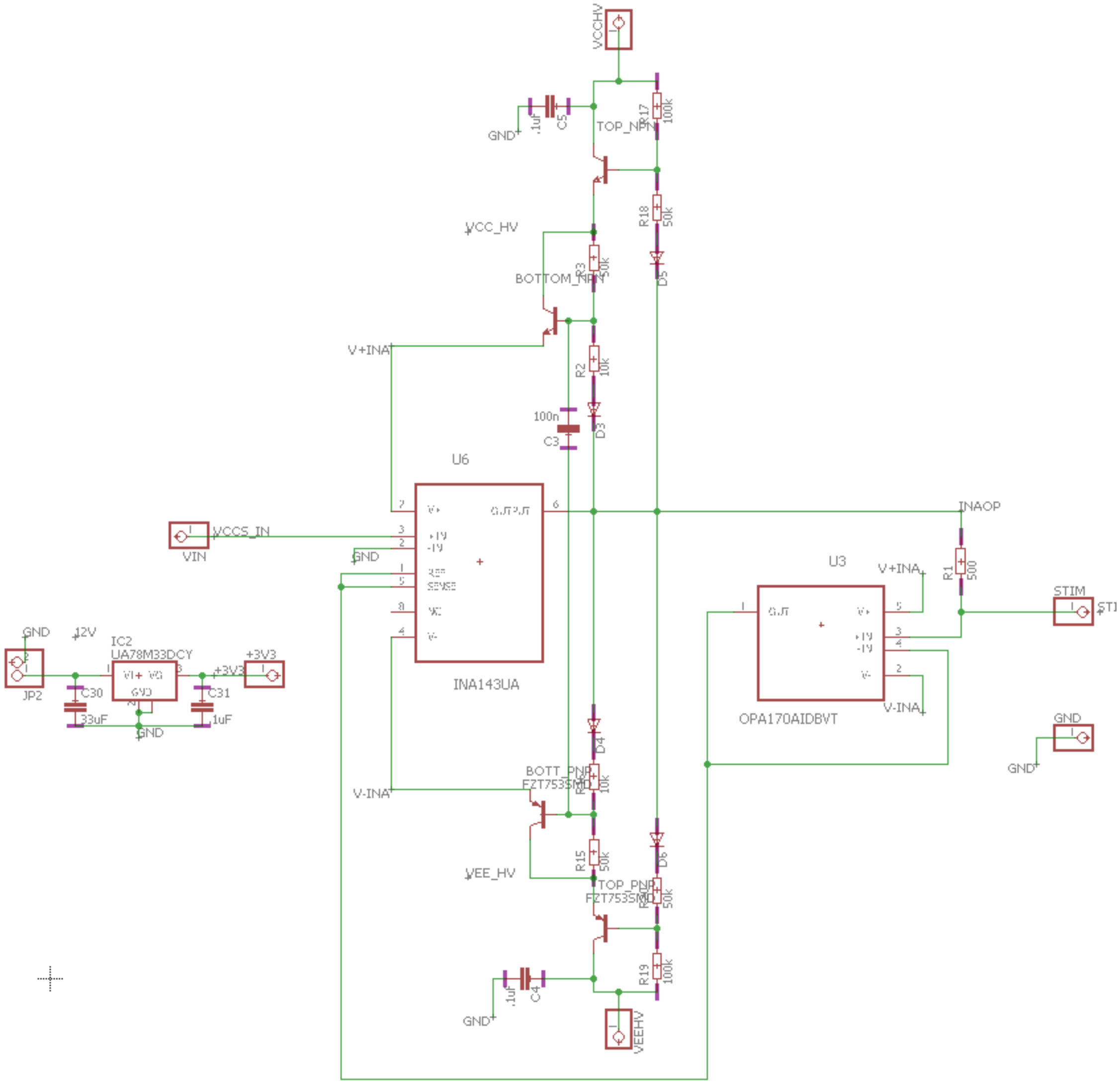

Figure 2: Constant Current Controller

Figure 2 shows the design of the voltage to current converter. This stage of the circuit directly interacts with the user’s skin by producing high voltage current pulses. The converter operates using a Howland current source implemented with standard off the shelf op-amps. A number of different circuits can be used to create a voltage to current source; we chose the Howland current source due to its fast rise times and linearity when tracking voltage references. Because skin resistances can be in the hundreds of kiloohms, our current source needs a high compliance voltage; to achieve this, we power the Howland current source with a bootstrap cascade, which sweeps the supply rails of the op-amps as a function of the output voltage. The Howland current source has two modifications, which we adapted from Caldwell [8]. The first is a commonly implemented modification which buffers the output of the traditional Howland current source for more robust operation. The second is to connect the REFB and REFA pins to the output of the buffer, which deviates slightly from the classic Howland topology without changing the input/output relationship; this was done to allow the +IN and -IN pins on our difference amplifier (INA149, TI) to be used, thus allowing us to take advantage of the chip's high common mode rejection. This effect could have also been achieved using an external resistor, but the former method slightly reduces component count and cost without changing the input/output relationship of the device. Solving the system for the relationship between V_{in} and I_{out} yields:

$$\frac{V_{in}}{R_{gain}} = I_{out} \qquad \text{(Eq 1)}$$

Where Vin is generated from the DAC, R_{gain} is R_1 in the above schematic, and I_{out} is the steady state output current. The derivation of this equation uses an approximation of an ideal operational amplifier, and therefore only captures steady state behavior and not the transient controller response, which we found to be negligible. In our device, the gain resistor value is 665Ω, allowing the min/max current for the device to be (slightly more than) +/-15mA.

The second component is the bootstrap network, which we adapted from both Brown [7] and Caldwell [8]. This network allows the compliance voltage of the device to be significantly increased, without having to resort to expensive high voltage operational amplifiers. The bootstrap network works by sweeping the op-amp supply rails as a linear function of the output voltage. Our device uses a cascaded bootstrap network, where the high voltage rails are stepped down in two stages before reaching the INA149 and OPA170. The high and low voltage networks are mirrored NPN/PNP networks; a close-up of the high side bootstrap cascade is pictured in Figure 3:

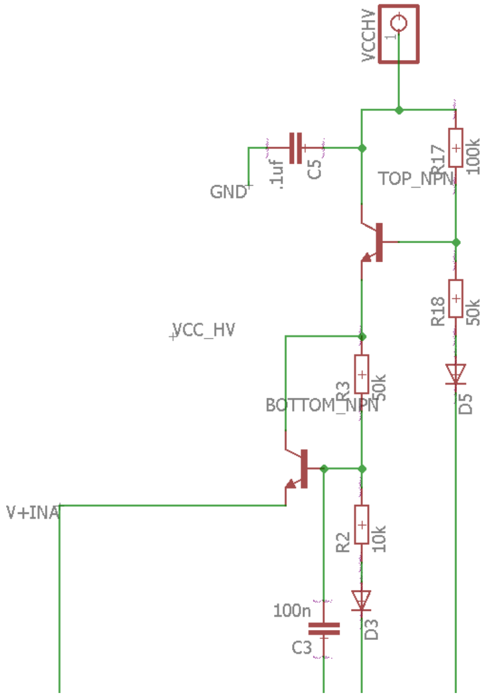

Figure 3: High side bootstrap cascade

In order to properly maintain the rail voltages of the constant current controller, the resistors of the bootstrap network needed to be properly tuned. The supply voltages produced by the bootstrap cascade (V_p and V_n) is given by the following equations:

$$V_p = \frac{(\frac{(V_{cc}-.6)R_1+V_{out}R_2}{R_1+R_2} - .6)R_3 + V_{out}R_4}{R_3 + R_4} \qquad \text{(Eq 2)}$$

$$V_n = \frac{(\frac{(V_{ee}+.6)R_5+V_{out}R_6}{R_5+R_6} + .6)R_7 + V_{out}R_8}{R_7 + R_8} \qquad \text{(Eq 3)}$$

Where V_p is the positive op amp supply rail and V_n is the negative supply rail.:

$$R_1 = R_5 = R_4 = R_8 = 50K \qquad \text{(Eq 4)}$$

$$R_2 = R_6 = 100K \qquad \text{(Eq 5)}$$

$$R_3 = R_7 = 10K \qquad \text{(Eq 6)}$$

An aggressive upper bound on our power supply rails is:

$$V_{cc} = 250V \qquad \text{(Eq 7)}$$

$$V_{ee} = -250V \qquad \text{(Eq 8)}$$

Substituting these values, we come to the final result that:

$$V_p - V_n = 21.9556V \qquad \text{(Eq 9)}$$

Which holds regardless of the value of V_{out} (i.e. V_{out} terms cancel) The above relationship holds assuming V_{out} has a value between the two supply rails, which is always the case in a practical scenario.

The maximum power supply range of the INA149 is 40V_{pp}, and the power supply range for the OPA170 is 36V_{pp}; 21.96V is well within this range, ensuring that the bootstrap network successfully protects the devices to which it supplies power by not exceeding their maximum allowable power supply voltage.

2.3 Power Supply

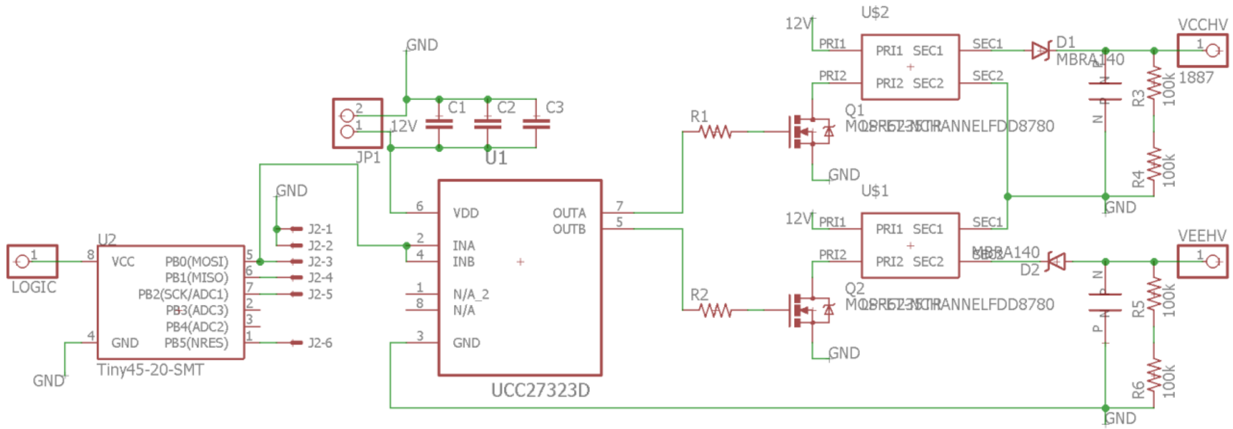

Figure 4: Power supply schematic

Figure 4 depicts the circuit design of the high voltage power supply. Fundamentally, this device is responsible for converting DC battery voltages between 9-12V (depending on the battery chemistry used) to +/-200V. A number of different switched-mode DC-DC converter topologies were considered for this module, including a standard boost converter, and even a modified boost converter with a voltage multiplication stage [12]. We concluded that a flyback topology was the ideal choice given the magnitude of the gains we needed, and the space available to achieve them. The biggest practical concern with flyback converters is the expense and availability of a suitable transformer; we selected the LPR6235 transformer manufactured by Coilcraft, which is small and inexpensive.

Our design drives two 1:20 turns ratio LPR6235 transformers with high current MOSFETs. The output of one transformer is rectified with high voltage schottky diodes such that the output voltage is positive, and the other is rectified such that the output voltage is negative. We use high valued bleed resistors on the output to stabilize the output of the transformer, approximately 1MΩ split into two resistors. The switching MOSFETS are driven via a dual MOSFET driver with an ATTINY45 microcontroller as the switching source, to allow us to programmatically control the power dissipated in the primary coils of the transformers.

Our design originally used more inexpensive ZXGD3005 MOSFET drivers; however, we discovered that these devices draw an abnormal amount of current on their input pin (up to 1A worst case) [11]. This property resulted in our microcontroller browning out/shutting down while trying to supply current to the drivers, which will be the case in most applications of this device if the input is not buffered. In the interest of achieving a functional device, we switched to the more expensive but higher performing UCC2732D dual MOSFET driver; however future versions of this device will likely include a modification which allows for the use of less expensive MOSFET drivers.

2.4 Pressure Sensor

The pressure sensors we designed work using inexpensive barometric pressure sensors. The sensors we use (MPL3115A2, NXP) consist of a small strain gauge and digital logic embedded in a metal case. There is a small opening in the case which exposes the strain gauge to open air. When silicone is poured over this hole and sealed with a vacuum pump, the sensor acts as a sensitive contact pressure sensor. Our design uses clusters of up to three of these sensors on flexible PCBs, with one PCB per finger in the hand. In our demonstration, we only have one cluster of three sensors, which directly connect to the DAC unit over I2C.

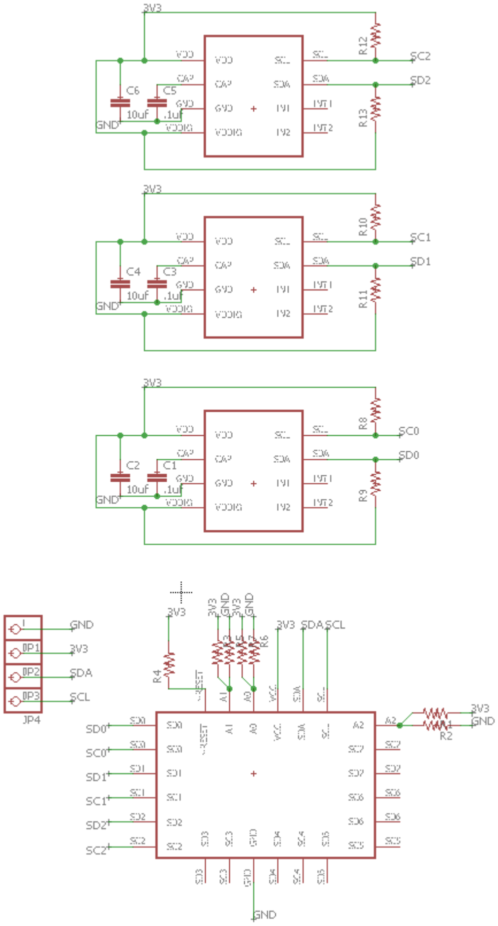

Figure 5: Pressure sensor schematic

Figure 5 shows the schematic capture for the flexible pressure sensor PCB. The pressure sensor PCB consists of an I2C mux and three MPL3115A2 barometric pressure sensors. Each of these barometric pressure sensors has a fixed I2C address; therefore in order to use multiple sensors simultaneously, an I2C mux is required. The I2C mux has a base address which can take up to eight values, based on the value of three address pins, allowing up to eight sets of these three fingers to operate on one I2C bus at a time.

Due to the mechanical construction of the pressure sensors, there is a significant amount of drift and hysteresis present in their data. To compensate for this, we implemented a time domain filter designed by PSYONIC in our source code which normalizes the data and compensates for drift.

2.5 DAC

The primary role of the DAC board is to provide voltage references to the constant current controller module, which produces a proportional steady state current. The DAC produces up to eight voltage outputs which can range between -10V to 10V. This board reads in pressure sensor data, applies a time domain filter to the data, performs the calculations necessary to produce the correct tracking voltage, and sequences the voltage waveform to send to the constant current controller. In future implementations of this system where the pressure sensors lie in the fingertips of an actual prosthesis, the data acquisition and time domain filter may be performed by a microcontroller present in the palm of the hand instead, which would send the relevant data to the microcontroller; however, the microcontroller we selected for the DAC module is powerful enough to handle both functions. The actual waveform we send can be controlled programmatically. We use a waveform commonly referred to as ‘biphasic’ in the context of electrical stimulation, which is simply a square wave that has a positive phase and a negative phase. Our waveforms have a fixed frequency of 50Hz and a duty cycle of 1%; both of these parameters can be changed to modify the sensation intensity alongside the waveform amplitude, but we found that changing only the amplitude of the pulses was sufficient to send expressive stimulation.

The schematic of the DAC microcontroller breakout is shown in Figure 6. We use a MK20DX256VLH7 microcontroller, and our breakout is based on the open source schematics for the teensy 3.2 [9]. The microcontroller communicates over SPI to a dedicated eight channel DAC chip (DAC108S085, TI), and over a single I2C bus to the pressure sensors. We program the microcontroller over USB, using a dedicated bootloader sold by PJRC; the same USB port can be used as a USB-serial port, which we use to run a simple terminal-based user interface.

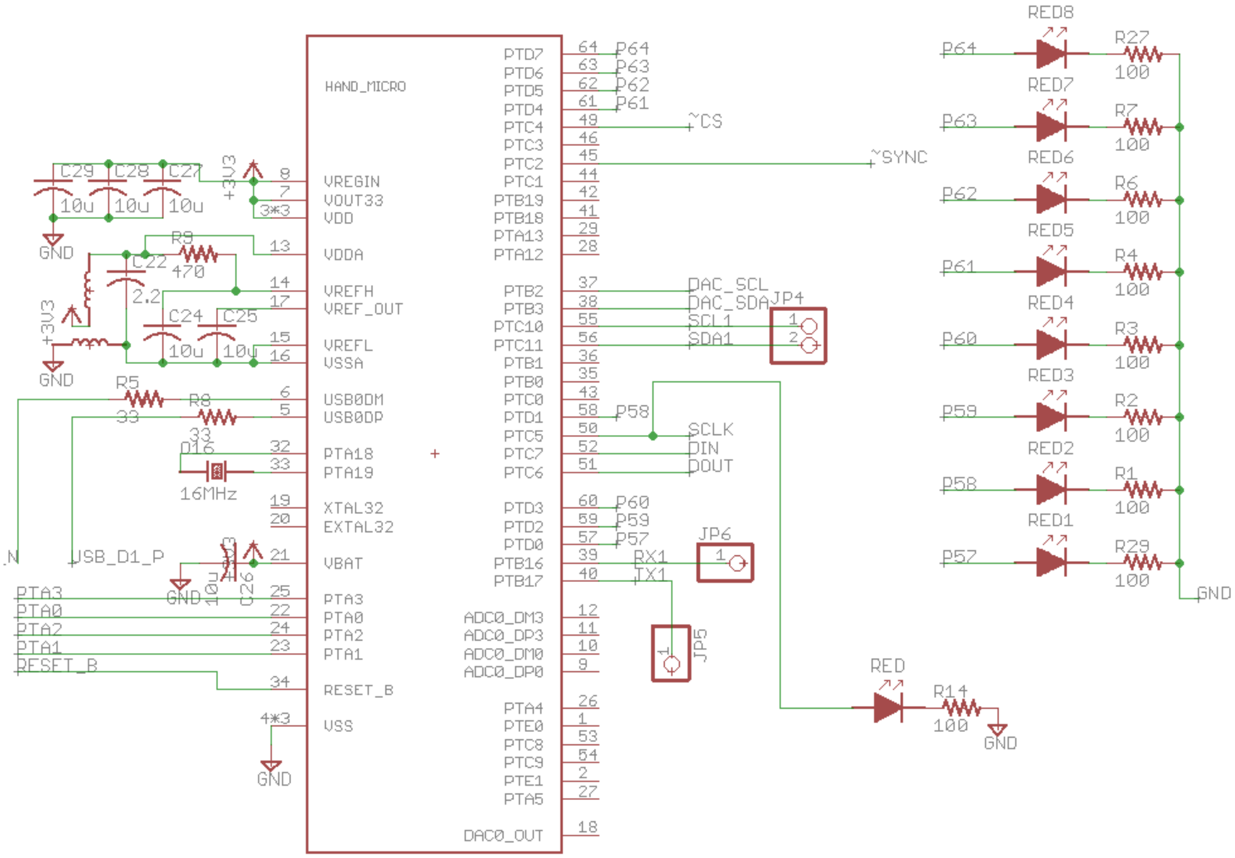

Figure 6: DAC board schematic: microcontroller and status LEDS

In addition to the base microcontroller breakout and headers for I2C peripherals, we added an array of eight status LEDs. These LEDs were added to provide additional feedback about the pressure sensor data, both for debugging and general use. Our design produces a ‘synthesizer’ effect with them, but there are many potential uses for these LEDs.

Figure 7 shows a schematic depicting the hardware responsible for producing the actual tracking reference voltages. As mentioned before, the central microcontroller communicates over SPI to the DAC chip. The DAC chip has eight channels, and produces voltages between 0V and 3.3V. To produce output voltages within the range we need for constant current control, -10V to 10V, we implemented a post-amplification stage which first “centers” the DAC output, producing a voltage between -3.3V and 3.3V, then amplifies the DAC output with non-inverting amplifiers to produce an output between -10V and 10V.

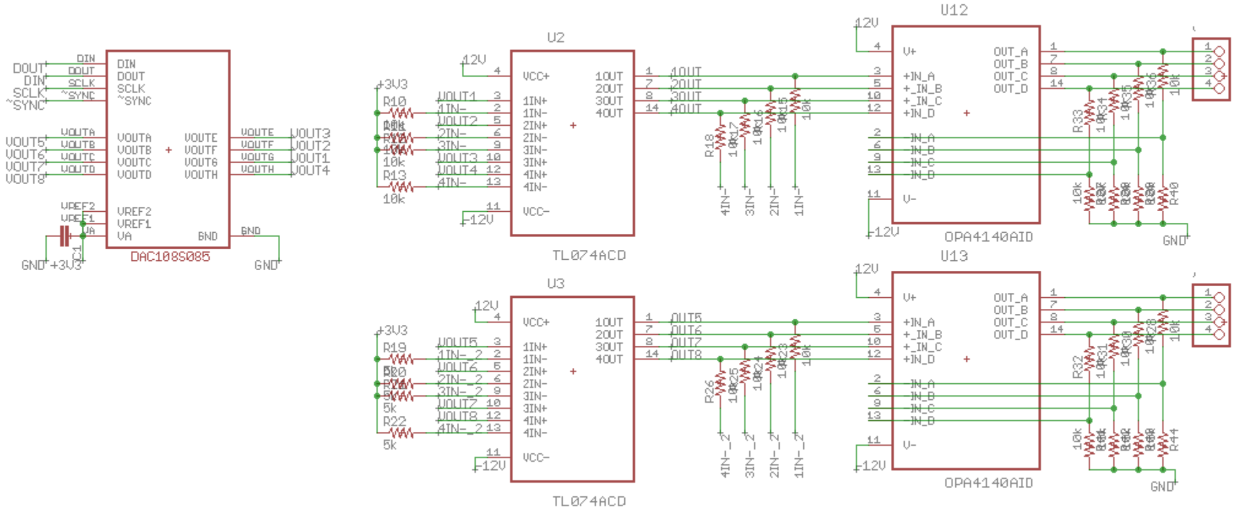

Figure 7: DAC board schematic: DAC and post-amplifiers

The amplifiers in Figure 7 need a positive and negative supply voltage to function as described. A simple approach to achieving this is to use two batteries in series; however, because we wanted to reduce the number of batteries we use as much as possible, we elected to use a switched-mode converter to invert our main power signal (9-12V). The output stage uses rail-rail amplifiers, so if our battery voltage V_{bat} is less than 10V, our output range will be exactly $+V_{bat}$ to $-V_{bat}$. Figure 8 shows the schematic for the power management system for the DAC.

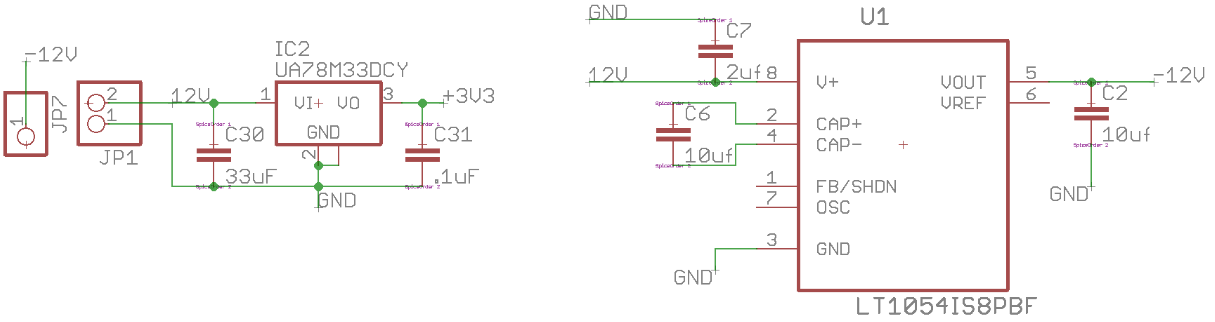

Figure 8: DAC board power management schematic

The inverter used is the LT1054 by Texas Instruments, a switched capacitor converter in a single chip solution. Also depicted in the above schematic is a simple linear regulator, which supplies 3.3V to all logic on the DAC board, as well as the pressure sensors via a header.

2.5 Software

Figure 9 shows the software flow for the stimulator. The software begins by acquiring the minimum and maximum current values for the subject. This process is performed using a simple terminal interface on a computer; the user sends keyboard commands to the device over a USB-serial interface to control the intensity of a calibration waveform. The minimum intensity is recorded when the user barely feels the stimulation and the maximum is recorded when the user feels a strong stimulation intensity.

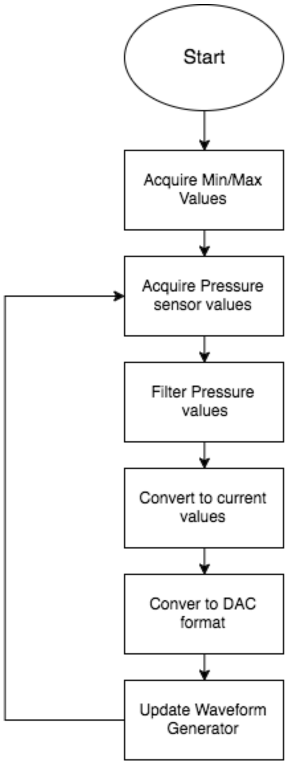
Start
Acquire Min/Max Values
Acquire Pressure sensor values
Filter Pressure values
Convert to current values
Conver to DAC format
Update Waveform Generator

Figure 9: Software Flowchart

Once the minimum and maximum intensities for all in-use channels are recorded in software, the pressure sensor values are polled, and their values are mapped to corresponding stimulation channels. In order to obtain useful pressure information, the pressure sensors must be post-processed to remove drift. We use a filter designed by PSYONIC in our design, which uses the mean and standard deviation of the data over a buffered range of samples to update the estimated minimum pressure value. This value represents the value read by the pressure sensor when no mechanical pressure is being applied. When the buffer of n samples is first filled, the minimum value is updated with the mean of the pressure sensor data obtained in that buffer. From then on, the buffer is updated in a circular fashion, and the minimum value is updated only if the current mean is less than 1.1 times the current minimum value and the current standard deviation is less than 1.1 times the standard deviation of the minimum value. Since the pressure sensors can be saturated during normal operation, the maximum pressure value is pre-recorded in software. The pressure data is then normalized (Equation 10).

$$p_{norm} = \frac{p - p_{min}}{p_{max} - p_{min}} \quad \text{(Eq 10)}$$

Once the pressure data is obtained, the DAC is responsible for producing a corresponding voltage reference. For a channel j, this is performed using the following equations. First, the maximum stimulation value is used to map the normalized pressure data to a current (Equation 11).

$$I_j = I_j^{max} p_{norm} \quad \text{(Eq 11)}$$

If the resulting current is above the minimum current threshold, the program proceeds; otherwise, a pulse with amplitude 0 is sent. To achieve the desired current on the output, the above value needs to be transformed twice more; the first time to produce a desired tracking voltage (Equation 12).

$$V_j = \frac{I_j}{665} \quad \text{(Eq 12)}$$

Where 665 is the gain resistor used in the constant current controller. Finally, the software needs to produce a 10-bit digital value which will be sent over SPI to the DAC, which will control the actual output reference voltage. The final linear transformation is given by Equation 13:

$$D_j = \frac{1023V_j}{20} + 512 \qquad \text{(Eq 13)}$$

Once the waveform amplitude is achieved in the digital output space, the actual waveform needs to be sequenced. This is done asynchronously using timer interrupts.

2.6 Physical Design

Physical layout is an important factor in our design. The entire device needs to fit inside a prosthetic socket, alongside additional electronic hardware responsible for EMG acquisition and hand control. An example socket is depicted in Figure 10. The stimulation electronics themselves are quite small; the DAC board is the largest at approximately 60x28mm, and the power supply and constant controller boards occupy only 43x21mm, which leaves plenty of room for multiple channels to fit inside a typical socket.

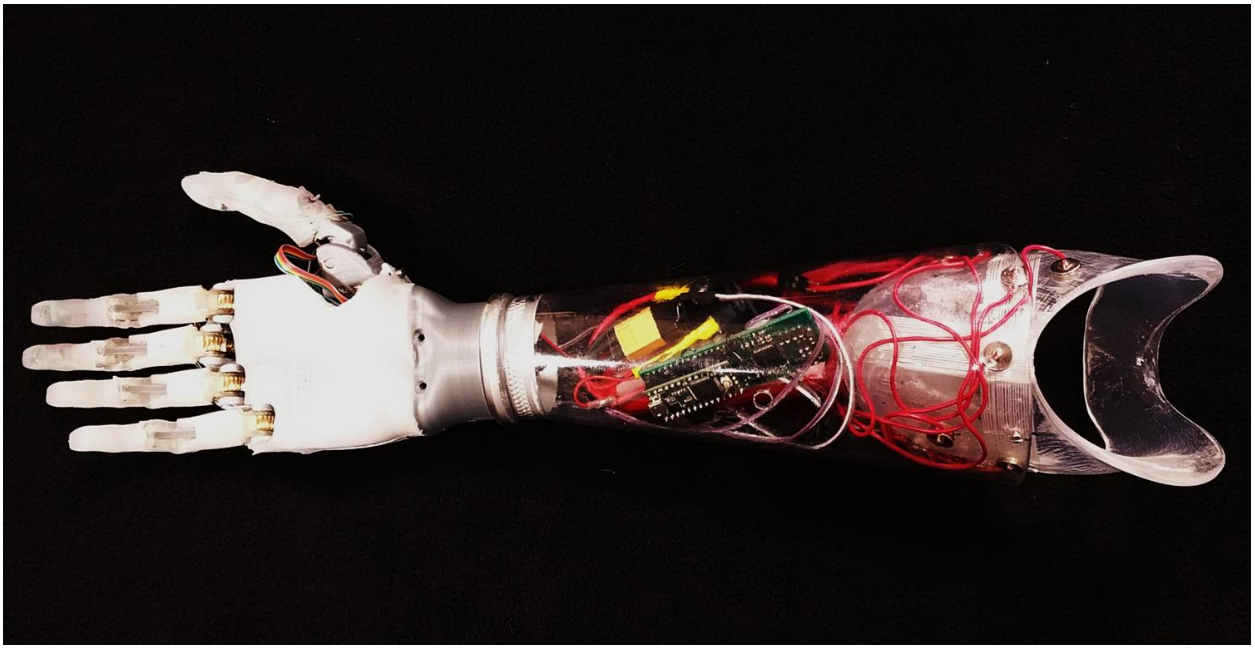

Figure 10: Example socket (right) and PSYONIC's myoelectric prosthetic hand (left)
(Photo credit: PSYONIC)

The pressure sensors are designed to integrate directly into the fingers of PSYONIC's prosthetic hand. The shape of these boards was designed in CAD software by Kyung Yun Choi, and the circuitry was laid out using that pre-defined layout. Figure 11 shows the CAD model of the internal bone structure of the finger with a mounted pressure sensor PCB.

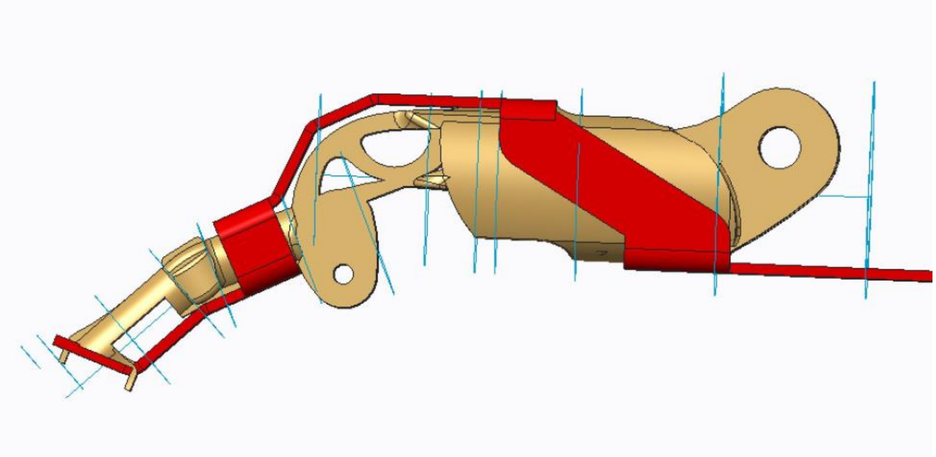

Figure 11: Compliant finger with board outline
(Photo/Finger Design credit: PSYONIC, Kyung Yun Choi)

The populated pressure sensor PCB is shown in Figure 12, both outside and inside a finger. We arranged the sensors in groups of three per board, with two sensors placed on the fingertip, and one on the lateral side of the finger. We anticipate the lateral side only being populated for the index finger, since that site is less relevant for the remaining fingers. Each of the fingers in the current PSYONIC hand are identical, which allows up to four of these PCBs to mounted per hand.

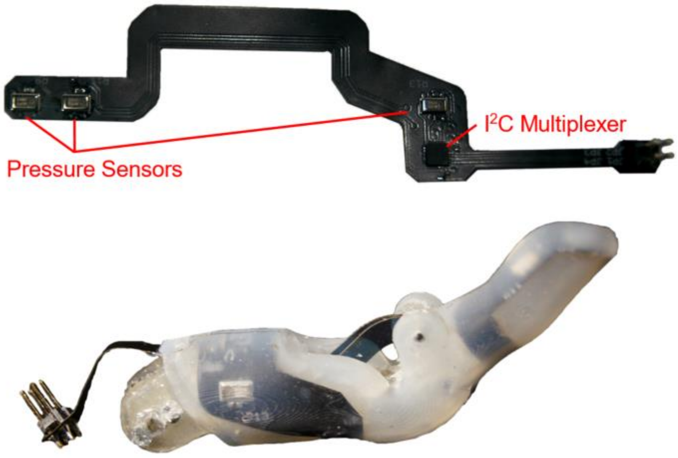

Figure 12: Pressure sensor board layout

The coupled constant current controller and power supply units, DAC, and pressure sensors can all function independently as isolated units; the modular nature of the design means that channels can be added and removed as desired with no loss of overall functionality. This lends itself well to the inconsistent nature of prosthetic sockets; due to variations in the length and size of each amputee's residual limb, sockets can vary significantly in size. Therefore it is advantageous to be flexible in the placement of each module, and to have control over the number of channels and therefore occupied space, to allow the device to conform to different socket shapes.

We designed and fabricated 3D printed enclosures for the device. We chose to use 9V batteries in our implementation due to their ubiquity and stable chemistry. However, 9V batteries have low energy capacity, and as a result we mounted one 9V battery in each case to power each stimulation channel. Each 9V battery occupies a significant amount of space, so future versions will likely use a single lithium polymer battery mounted externally to power the channels, thus drastically reducing the total space occupied by the device.

3 Verification

3.1 Constant Current Controller

To verify the target electrical specifications of the constant current controller, we tested it using both monophasic (step response) and biphasic waveforms with varying amplitudes across a number of different resistive loads. Our most important requirements for the constant current controller are that it produces constant current signals, that the compliance voltage can reach +/-150V, and that the peak current can reach +/-15mA.

Figure 13 shows our verification data for the constant current requirement. This figure shows the voltage and current step responses of the constant current controller when connected to a series of different resistances, and demonstrates that the output voltage varies with resistance but the current remains constant.

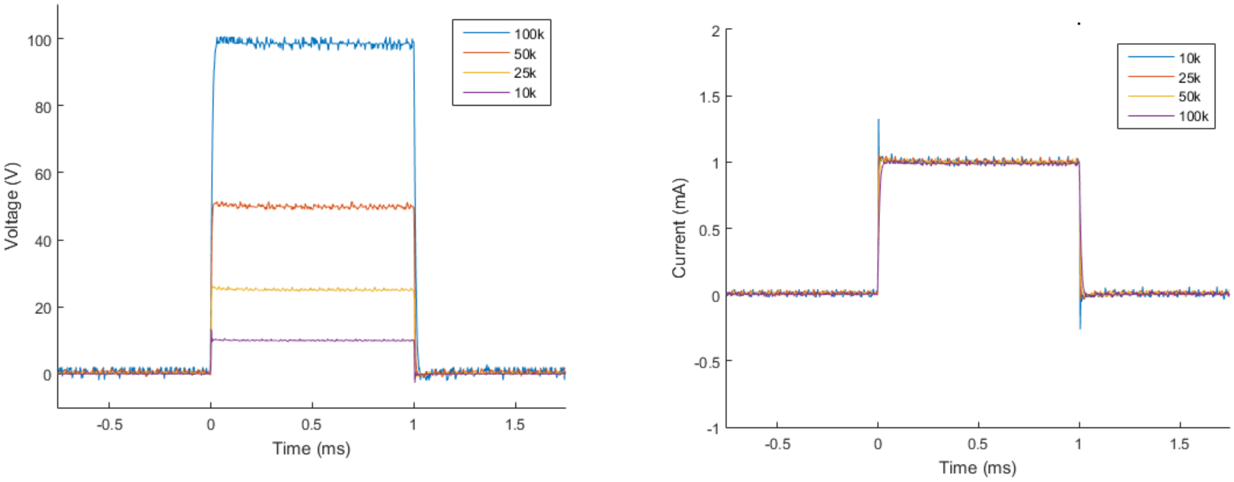

Figure 13: Voltage drop (left) and measured current (right) of a series of load resistances

To verify that we can produce outputs with a compliance voltage of +/-150V, we sent a biphasic signal of 1mA across a 150kΩ resistor and measured the voltage with an oscilloscope. To verify that we satisfy our peak current requirements, we sent a 15mA signal across a 5kΩ resistor, recorded the voltage drop, and divided out the 5kΩ resistor; the results of both of those tests are shown in Figure 14.

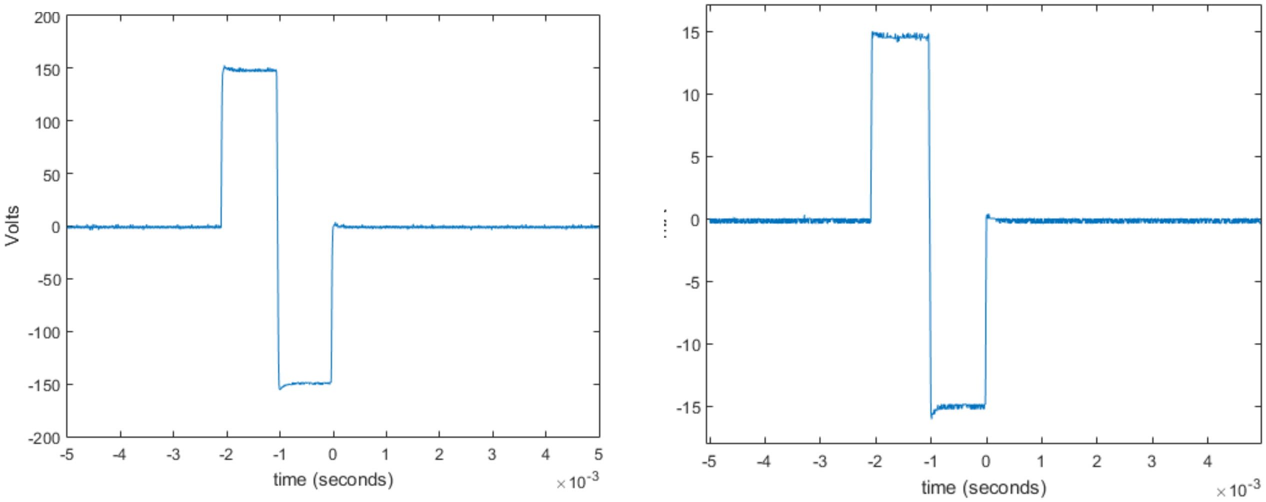

Figure 14: Voltage drop of a 1mA signal across a 150k load (left), +/-15mA signal across a 5k resistor (right)

Another important requirement for this module is noise. To verify that our stimulation noise was under our target value of $2V_{pp}$, we measured the output of a stimulation channel with an oscilloscope while connected to a 10kΩ load, and found that the output noise was consistently below $1.5V_{pp}$. This result can be clearly seen in Figure 15.

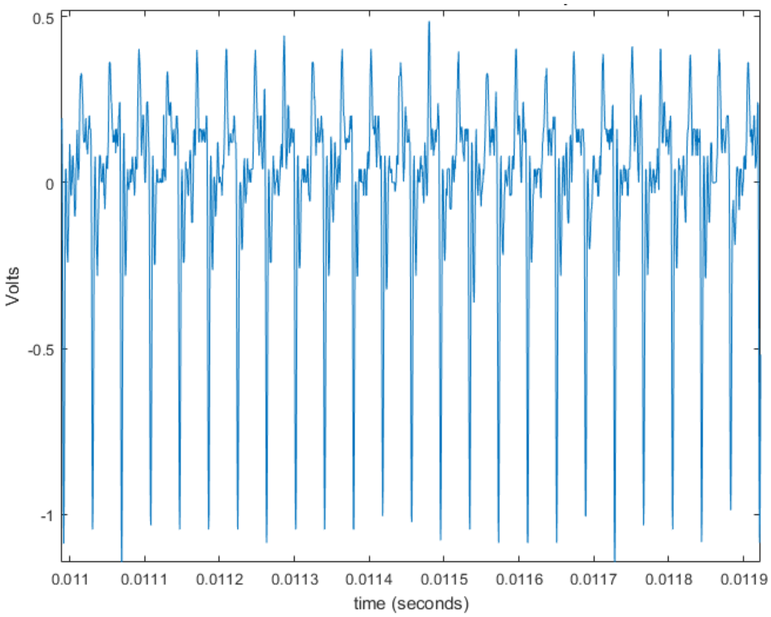

Figure 15: Stimulation output noise across a 10k load.

3.2 Power Supply

We verified the performance of the power supply independently by measuring the output voltage under a no-load condition. The resulting output was stable, low noise +/-200V$_{dc}$, which can be seen in Figure 16. We also analyzed the overall quiescent power consumption of the power supply and constant current controller, finding it to be approximately .5329W, which was well under our target value of 1W.

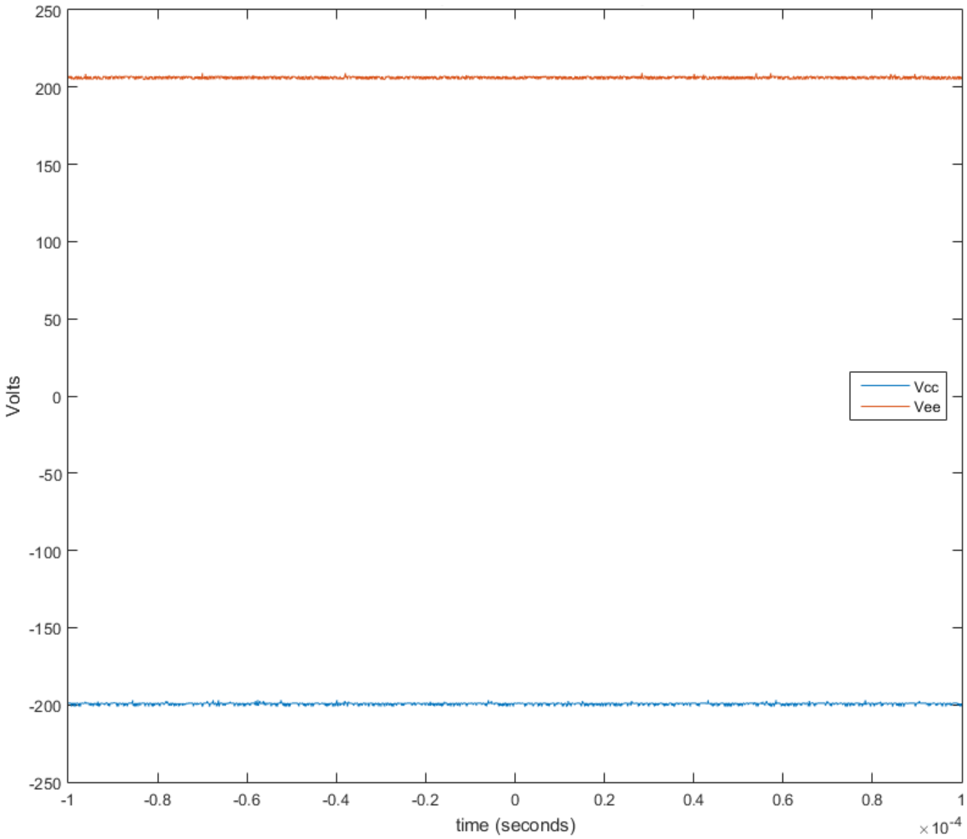

Figure 16: Power Supply Output Rails, No load

3.3 Pressure Sensor

We verified the performance of the pressure sensors and time domain filter by logging the information using a USB-serial connection, and plotting the data in MATLAB. An example of this plot is shown below in Figure 17. We found with the implementation of the time domain filter, our pressure sensor could dynamically compensate for changes in baseline drift, and as a result was able to control the stimulation output without introducing errors.

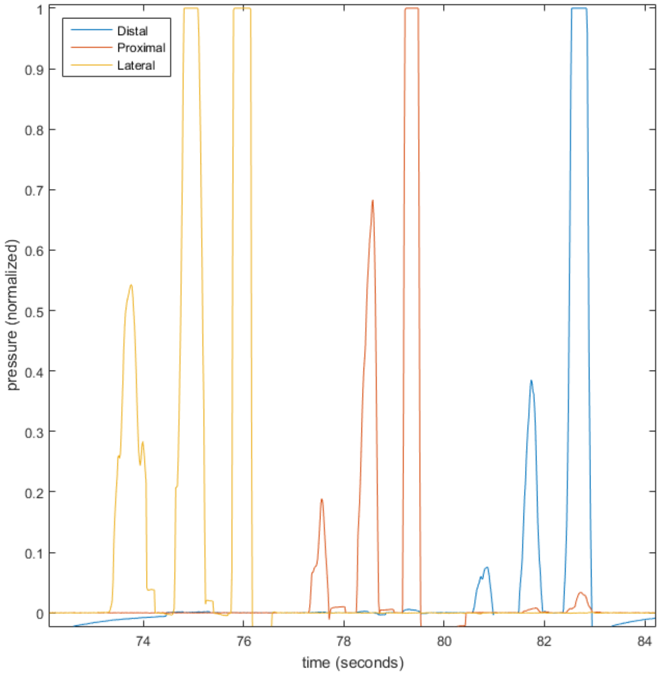

Figure 17: Pressure sensor data for all three sites

3.4 DAC

We verified the performance of the DAC module by programming it to output a biphasic waveform on each of the eight channels, then measuring the output with an oscilloscope. We also confirmed that we were able to change the amplitude of these pulses with both the pressure sensor and through the serial interface with an oscilloscope before connecting the output to our skin.

4. Costs

We estimate our development costs to be $30/hour, 12 hours a week for two people. For 16 weeks, the total development cost is:

$$2\frac{\$30}{hr}\frac{12hr}{wk}16wks = \$11520 \tag{Eq 14}$$

Our estimated component cost for each of the four modules is detailed in Appendix A. The resulting cost is $77.89. We anticipate the combined unit cost of all four PCBs to be <$20, bringing the total device cost at low volume to approximately $97.89.

5. Conclusion

Our project was an overall success. We were able to verify every one of our requirements, including the less essential ones listed in Appendix B. The biggest problem with the device in its current state is that it is bigger than it could be; this is due to the fact that we chose 9V batteries to power our stimulation channels because of their stable chemistry. Using a larger capacity lithium-ion battery instead of multiple 9V batteries would compensate for this problem with no loss of functionality.

The most apparent safety risk in our project is the delivery of a dangerous shock; this hazard is endemic to devices of this nature. Throughout our project, we paid close attention to the IEEE Code of Ethics #1, which is the most relevant to this project; electrical stimulation has significant potential for rehabilitative care, but if mishandled can result in serious injury [6]. We took measures to ensure safe use by designing power limitations into our device, and by thoroughly verifying functionality on an oscilloscope before connecting our device to a human being. All human subject experiments with our device have been approved by the University of Illinois at Urbana-Champaign Institutional Review Board #13920.

The device is very easy to set up and the operation is intuitive. In an informal test, we verified a user's ability to localize various stimulation sites (i.e. discriminating between what electrode corresponds to what site on the finger). The cost of the device is one of the most compelling aspects of our project; we can provide a complete haptic feedback system for less than $100. Future work for this project will be to achieve multiple channels of stimulation using multiplexing techniques, which sacrifices control of the phase of the stimulation signals, but saves on space, cost, and power consumption. In the long term, our device will be used for research with amputees to evaluate its performance, and for experiments with sensation quality control.

References

[1] Biddiss E, Beaton D, Chau T. Consumer design priorities for upper limb prosthetics. Disabil. Rehabil. Assist. Technol. 2(6), 346-357 (2007).

[2] Kyberd PJ, Wartenberg C, Sandsjö L et al. Survey of upper-extremity prosthesis users in Sweden and the United Kingdom. J. Prosthet. Orthot. 19(2), 55-62 (2007)

[3] A.I Lauer, K. Longenecker Rust, R. O. Smith. Factors in Assistive Technology Device Abandonment: Replacing “Abandonment” with “Discontinuance”. (2015) [Online]. Available: http://www.r2d2.uwm.edu/atoms/archive/technicalreports/tr-discontinuance.html. [Accessed: 07- Feb- 2017].

[4] C. Antfolk, M. D’Alonzo, B. Rosén, G. Lundborg, F. Sebelius, C. Cipriani, Sensory feedback in upper limb prosthetics. (2013) [Online]. Available: https://pdfs.semanticscholar.org/5cf2/d32093fe0d37de39c399ed1d6cef9f6ae884.pdf [Accessed: 07- Feb- 2017].

[5] H. Kajimoto, “Electro-tactile Display: Principle and Hardware”, in Pervasive Haptics, Tokyo, Japan; Springer, 2016, ch. 5 sec. 5.3.1, pp. 89.

[6] Ieee.org, "IEEE IEEE Code of Ethics", 2016. [Online]. Available: http://www.ieee.org/about/corporate/governance/p7-8.html. [Accessed: 8-Feb- 2017]

[7]G. King and T. Watkins, "Bootstrapping your op amp yields wide voltage swings," in http://joebrown.org.uk/, 1999. [Online]. Available: http://joebrown.org.uk/images/DualPSU/BootstrappingOpAmps.pdf. [Accessed: Feb. 21, 2017]

[8] J. Caldwell, "A High-Voltage Bidirectional Current Source," in Texas Instruments, 2013. [Online]. Available: http://www.ti.com/lit/ml/slyy054/slyy054.pdf. [Accessed: Feb. 21, 2017]

[9] P. Stoffregen, "Teensy and Teensy++ schematic diagrams," 1995. [Online]. Available: https://www.pjrc.com/teensy/schematic.html. [Accessed: Feb. 24, 2017.]

[10] Texas Instruments, “DAC108S085 10-Bit Micro Power OCTAL Digital-to-Analog Converter with Rail-to-Rail Outputs,” DAC108S085 datasheet, Aug. 2007 [Revised March. 2013].

[11] "25V 10A GATE DRIVER IN SOT26", *A Product Line of Diodes Incorporated*, 2011. [Online]. Available: https://www.diodes.com/assets/Datasheets/ZXGD3005E6.pdf. [Accessed: 02- May- 2017].

[12] B. McCoy, "Design Note – DN05019/D 200V Boost Regulator", 2011. [Online]. Available: http://www.onsemi.com/pub/Collateral/DN05019-D.PDF. [Accessed: 03- May- 2017].

Appendix A: Component Cost Breakdown

Part	Quantity	Cost
LPR6235 (Transformer)	2	$1.40
1uf 0805	3	$.30
6 pin FFC connector	1	$1.07
STD15NF10 (N-MOSFET)	2	$2.40
10uF 250V Capacitor (Custom package)	2	$1.58
MOSFET Driver	2	$1.18
ATTINY45	1	$1.11
10uF 0402 Capacitor	3	$.54
MPL3115A2 (Barometric pressure sensor)	3	$12.96
TCA9548A (I2C Mux)	1	$1.50
10uF 0603 Capacitor	10	$.99
2.2uF 0603 Capacitor	2	$0.20
33uF 0603 Capacitor	1	$0.13
MK20DX256VLH7 (Main Microcontroller/DAC microcontroller)	1	$6.50
UA78M33C (3.3V regulator)	2	$1.16
9 pin FFC connector	1	$1.23
16 Mhz Crystal	1	$0.75
DAC108S085 (DAC chip)	1	$7.59
600 Ohm 0603 Ferrite Bead	2	$0.40
LT1054 (Voltage Inverter)	1	$4.27
TL074 (quad op amp)	2	$1.02
666 Ohm 0603 Resistor	1	$0.10
Gen Purpose SMA Diode	4	$0.96
INA149	1	$6.96
300V NPN SOT-223 Transistor	2	$1.90
300V PNP SOT-223 Transistor	2	$2.04

1KV SMA Schottky Diode	2	$0.94
0 Ohm 0603 Jumper	10	$0.10
1M 1206 Resistor	10	$1.80
0 Ohm 0201 Jumper	10	$.26
1K 0402 Resistor	10	$0.11
.1uF 0402 Capacitor	10	$0.12
33 Ohm 0402 Resistor	10	$0.17
100 Ohm 0402 Resistor	10	$0.12
10K 0402 Resistor	25	$0.19
470 Ohm 0402 Resistor	25	$0.19
LED 0603	10	$1.96
10K 0603 Resistor	10	$0.10
100K 0603 Resistor	10	$0.10
49.9K 0603 Resistor	10	$0.13
.1uF 0603 Resistor	10	$0.18
OPA170 (Op amp)	10	$12.58
Total Component Cost:	$77.89	

Appendix B: Requirements and Verification

Constant Current Controller:

Requirement	Verification	Points
1. Must be constant current. 2. Must be able to provide +/-15mA. 3. Compliance voltage must be at least +/-150V. 4. Must have fast rise times (<2us). 5. Must have noise that is not perceptible in the stimulation output (low ringing, good PSRR). Target noise is <2Vpp.	1. Connect resistors of varying impedances to the stimulator and measure the voltage drop. Verify the current waveform is consistent each of these resistive loads. 2. Provide the appropriate input voltage, measure the drop across a known resistance 3. Send +/-1mA across a 150k resistor, measure the voltage drop across this resistor and ensure it is +/-150V. 4. Send a square wave input signal, measure the stimulator rise time with an oscilloscope 5. Measure the noise with an oscilloscope	1. __________/20 2. __________/20 3. __________/20 4. __________/5 5. __________/5 Total: ______/70

Boost Converter:

Requirement	Verification	Points
1. Must be able to provide at least +/-200V. The input voltage can range from 9-12V, depending on the type of battery desired. The output need not be regulated. 2. Noise must be low enough that the current controller PSRR can compensate for it. Noise must be low enough to not have any physiological effect; an upper maximum is +/-2V. 3. When connected to the constant current source, the stimulator system will not dissipate more than 1W (quiescent), to ensure practicality in a mobile setting.	1. Measure the output with no load (bleed load) and verify the output voltage with an oscilloscope or multimeter 2. Check the noise with an oscilloscope. 3. Measure the voltage drop across a low value resistor in series with the battery when connected to the stimulator, which should send 0mA across some typical load resistance (10k). Log this voltage drop with an oscilloscope, and use the data to calculate power.	1. __________/20 2. __________/5 3. __________/5 Total:_______/30

DAC:

Requirement	Verification	Points
1. The chip must be SPI controlled; this is to allow the central microcontroller to be configured as either I2C master or slave, depending on whether it interfaces with the pressure sensors directly or through a different microcontroller. 2. The DAC PCB must be capable of producing 50Hz bipolar square pulses between -10V and 10V on all eight channels, with the same phase.	1. Check to make sure SPI communication works by measuring output waveforms with an oscilloscope. 2. Verify that the output waveform is correct with an oscilloscope.	1. __________/5 2. __________/20 Total :______/25

Pressure Sensors:

Requirement	Verification	Points
1. The pressure sensor data has manageable drift and hysteresis, if present; the pressure sensor data should be post-processed such that the output must not cause the baseline stimulation to drift enough to feel a difference (typical JND is .1mA).	1. Log the pressure sensor data into a file and plot it in matlab. Verify the post-processed output does not result in drift which would create a perceptible change in stimulation (JND .1mA).	1. __________/20